JHEP|Reports

CPEB4 modulates liver cancer progression by translationally regulating hepcidin expression and sensitivity to ferroptosis

Authors

M. Eugenia Delgado, Salvador Naranjo-Suarez, Marta Ramírez-Pedraza, …, Mark Boyle, Raúl Méndez, Mercedes Fernandez

Correspondence

mlobato@recerca.clinic.cat (M. Fernandez).

Graphical abstract

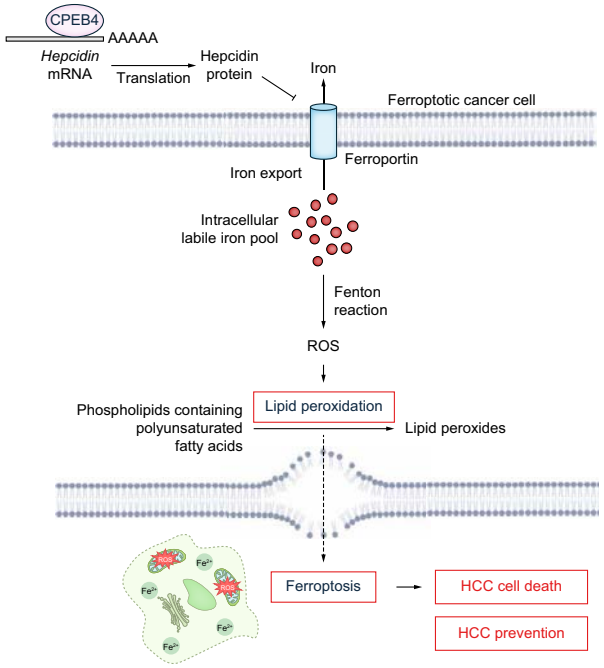

Highlights:

- RNA-binding protein and master translation regulator CPEB4 identified as a key player in hepatocellular carcinoma progression.
- CPEB4 regulates hepcidin expression, thereby modulating cancer cell sensitivity to ferroptosis, a specific form of cell death.
- This discovery reveals a novel translational regulatory mechanism in cancer biology with significant therapeutic potential.
- Further validation through human clinical studies is essential to confirm the role of CPEB4 in liver cancer.

Impact and implications:

This study addresses the pressing need for improved therapies in liver cancer, particularly given its increasing prevalence linked to obesity and metabolic-associated fatty liver disease. By uncovering the role of the RNA-binding protein cytoplasmic polyadenylation element binding protein 4 (CPEB4) in modulating iron regulation and cancer cell sensitivity to ferroptosis, our research highlights a new translational mechanism with potential therapeutic relevance. These findings are particularly significant for clinicians, researchers, and policymakers focused on advancing targeted treatments for hepatocellular carcinoma. If further validated in human clinical studies, targeting CPEB4-mediated pathways could help develop treatments that enhance cancer cell susceptibility to ferroptosis, offering a promising strategy for improving outcomes in patients with advanced liver cancer. Limitations of the study include the need for further clinical validation to confirm these preclinical findings in human disease contexts.

https://doi.org/10.1016/j.jhepr.2024.101296

Research article

JHEP|Reports

CPEB4 modulates liver cancer progression by translationally regulating hepcidin expression and sensitivity to ferroptosis

M. Eugenia Delgado[1,†], **Salvador Naranjo-Suarez**[1,†], **Marta Ramírez-Pedraza**[1,†], Beatriz I. Cárdenas[1], Carmen Gallardo-Martínez[1], Alexandra Balvey[1], Eulalia Belloc[2], Judit Martín[2], Mark Boyle[1], Raúl Méndez[2,3,*], Mercedes Fernandez[1,*]

JHEP Reports **2025**. vol. 7 | 1–13

Background & Aims: Liver cancer is a significant global health issue, with its incidence rising in parallel with the obesity epidemic. The limited therapeutic options available emphasize the need for a better understanding of the molecular pathways involved in its pathogenesis. While much of the previous research has focused on transcriptional changes, this study examines translational alterations, specifically the role of cytoplasmic polyadenylation element binding protein 4 (CPEB4), a key regulator of translation.

Methods: We analyzed publicly available patient databases and conducted studies using human and mouse liver cancer cells, xenograft and allograft models, mouse models of high-fat diet-related liver cancer, and CPEB4 knockout and knockdown mice and cell lines.

Results: Patient data analysis (n = 87) showed a strong correlation between low CPEB4 levels and reduced survival rates (p <0.001). In mouse models of diet-induced liver cancer (n = 10–15 per group), both systemic and hepatocyte-specific CPEB4 knockout mice exhibited significantly increased tumor burden compared with wild-type controls (p <0.05). *In vitro* studies using human and murine liver cancer cells (n = 3 biological replicates) demonstrated reduced sensitivity to ferroptosis upon CPEB4 depletion when induced by erastin or RSL3 (p <0.01). Mechanistically, CPEB4 deficiency suppressed hepcidin expression, leading to elevated ferroportin levels, decreased intracellular iron accumulation, and reduced lipid peroxidation (p <0.05).

Conclusions: This study uncovers a novel CPEB4-dependent mechanism linking translational control to liver cancer progression and ferroptosis regulation. Therapeutic strategies targeting CPEB4-mediated pathways hold promise for advancing treatment options in liver cancer.

Introduction

Liver cancer represents a significant global health challenge and remains a leading cause of cancer-related deaths, with advanced cases exhibiting poor prognosis and limited treatment options.[1] The rising incidence of liver cancer is particularly concerning as it correlates with the escalating obesity epidemic.[2] Obesity is closely linked to the development of metabolic-associated fatty liver disease (MAFLD), formerly known as non-alcoholic fatty liver disease, which is characterized by the accumulation of fat in the liver. MAFLD can progress to more severe forms, including non-alcoholic steatohepatitis, fibrosis, and ultimately, hepatocellular carcinoma (HCC).[3,4]

Evasion of cell death is a critical aspect of cancer growth and progression.[5] Traditionally, apoptosis has represented the most studied programmed cell death mechanism.[5] However, recent research has highlighted the importance of alternative pathways, such as ferroptosis.[6–9] Ferroptosis is an iron-dependent form of regulated cell death characterized by the accumulation of lipid peroxides.[6–9] Despite its emerging importance in cancer biology, our understanding of ferroptosis in liver cancer remains limited. Additionally, the underlying molecular mechanisms that determine the sensitivity of tumor cells to ferroptosis remain largely unknown. Elucidating these mechanisms could not only enhance our understanding of the basic processes driving liver cancer, but also unveil novel therapeutic targets.

Translational regulation of gene expression is pivotal in cancer development and progression.[9–14] However, our understanding of this aspect of gene expression regulation is limited, as the majority of previous studies have primarily focused on transcriptional control mechanisms. One crucial mechanism of translational control involves the cytoplasmic polyadenylation element binding (CPEB) family of RNA-binding proteins.[15–19] CPEB proteins regulate mRNA translation and stability by recognizing a cis-acting element known as the cytoplasmic polyadenylation element (CPE) in the 3′-untranslated region (UTR) of target mRNAs, subsequently modifying the length of their poly(A) tails.[20,21] The dysregulation of the CPEB-mediated translational control has been implicated in

* Corresponding author. Address: IDIBAPS, Rosselló Street 149, 08036 Barcelona, Spain. Tel.: +34-606958606.
E-mail address: mlobato@recerca.clinic.cat (M. Fernandez).
† Co-first authors.
https://doi.org/10.1016/j.jhepr.2024.101296

several diseases.[22–28] However, the specific roles of CPEB in liver cancer are not fully understood.

In this study, we addressed these knowledge gaps and demonstrated that translational control and ferroptosis play a major role in liver cancer. We found that CPEB4, the stress-regulated member of the CPEB family,[22–28] regulates liver cancer ferroptosis through the translational control of hepcidin. Our findings revealed that low CPEB4 protein expression correlates with poor prognosis, decreased survival, and increased rate of both tumor progression and severity in human and mouse HCC. Moreover, we found that CPEB4 deficiency promotes liver tumor growth; importantly, one of the notable mechanisms through which this is achieved is through the attenuation of ferroptosis via the hepcidin–ferroportin axis and the regulation of iron-dependent lipid peroxidation in liver tumor cells. These findings not only highlight the importance of CPEB4-mediated translation in liver tumor growth, but also introduce a novel mechanism for the regulation of ferroptosis sensitivity through CPEB4-mediated translational control. This knowledge has the potential to significantly advance our understanding of liver cancer pathogenesis and may lead to the development of new therapeutic strategies for this deadly disease.

Materials and methods

A detailed description of the Materials and methods can be found in the Supplementary material.

Animal models

Animals (*Mus musculus*, C57BL6/J pure and C57BL6/J-129S mixed backgrounds) were maintained under a standard 12-h light/dark cycle, at 23 °C, with free access to food and water. At 6 weeks of age, male mice were randomly assigned to either a high-fat diet (HFD) (60% fat, 20% protein, and 20% carbohydrates; D12492, Research Diets, New Brunswick, NJ, USA) or a normal diet (ND) (7.42% fat, 17.49% protein, and 75.09% carbohydrate; Research Diets). Mice were fed with HFD or ND for a period of 50 weeks. The procarcinogen diethylnitrosamine (DEN, 80 mg/kg; Sigma, St. Louis, MO, USA) was injected intraperitoneally into 16-week-old mice. From week 20 until the end of the protocol, 0.05% phenobarbital, a tumor promoter, was added into the drinking water. Protocols were approved by the Animal Ethics Committee of the University of Barcelona and the Catalan Government and followed the ARRIVE guidelines.

Generation of constitutive, inducible, and hepatocyte-specific CPEB4 knockout mice

To generate a Cpeb4 conditional knockout mouse (Cpeb4l$^{ox/lox}$), mouse embryonic stem cells carrying a βgeo (β-galactosidase gene fused to neomycin resistance gene) cassette in Cpeb4 intron-1 and loxP sites flanking exon-2 (clone EPD0060_4_E10; Sanger Institute, Cambridge, UK) were microinjected into developing blastocysts. The resulting positive chimeric mice (Cpeb4$^{+/loxfrt}$) were crossed with C57BL6/J mice. Subsequently, the βgeo-cassette was removed by mating with mice expressing the FlpO recombinase (Tg.pCAG-Flp), generating conditional knockout animals (Cpeb4$^{lox/lox}$). To obtain a ubiquitous and constitutive depletion of CPEB4, Cpeb4$^{lox/lox}$ mice were crossed with animals expressing DNA recombinase Cre under control of a human cytomegalovirus minimal promoter (B6.C-Tg(CMV-cre) 1Cgn/J). Excision of exon 2 of the Cpeb4 gene leads to a frame shift in the mRNA generating several new premature stop codons, resulting in mice that are deficient in CPEB4 protein (Cpeb4^{KO}). Offspring was maintained in a C57BL/6J-129S mixed background. To obtain a tamoxifen-inducible mouse line, conditional mice were crossed with Tg.Ubc-CreERT2 mice. Hepatocyte-specific Cpeb4 knockout mice (Cpeb4^{HKO}) were obtained by crossing Cpeb4l$^{ox/lox}$ mice with albumin-Cre transgenic animals. Offspring was backcrossed for five generations onto the C57BL/6J background. Routine genotyping was performed by PCR.

Generation of stable CPEB4 knockdown human liver cancer cell lines

To generate CPEB4 knockdown human liver cancer cell lines, short hairpin RNA (shRNA) encoding sequences were delivered to the HepG2 and Huh7 cell lines through lentiviral infection. Lentivirus were produced by transfection of 293T packaging cells with the plasmids psPAX2 (Addgene, Watertown, MA, USA), ENV (Addgene) and pLKO shCPEB4.4 (Sigma-Aldrich, St. Louis, MO, USA), using the liposome-based DNA transfection reagent LipoD293 (SignaGen, Frederick, MD, USA). The pLKO shCPEB4.4 vector carried a sequence specific for CPEB4 shRNA expression (5′-GCGTTATGTGTTGAACAGTAT-3′) and puromycin resistance marker. A scramble control RNA that does not recognize any region in the mammalian genome was used to obtain the wild-type (WT) cells (MISSION® pLKO.1-puro non-mammalian shRNA control plasmid DNA from Sigma-Aldrich was used). Media from transfected 293T cells was removed and replaced with fresh media every 24 h. The media were harvested 48 and 72 h post-transfection, filtered through a 0.22-μm filter (to use only the lentiviral particles) and used to infect HepG2 and Huh7 cells grown on 6-cm dishes. Efficiently infected tumoral cells were selected with 2 μg/ml puromycin to create stable CPEB4 knockdown HepG2 and Huh7 cells.

Cell viability assays

Viability assays were conducted using two well-established methods that assess cell viability based on different metabolic parameters: The MTT assay (3-(4,5-dimethylthiazol-2-yl)-2,5-diphenyltetrazolium bromide; Sigma) measures mitochondrial activity, providing an indirect measure of cell viability. Tumor cells were plated in a multiwell plate and treated with the ferroptotic cell death inducers erastin (Sigma) or RSL3 (Sigma), or with the ferroptosis-specific inhibitor ferrostatin-1 (Cayman Chemicals, Ann Arbor, MI, USA). MTT reagent, a yellow tetrazolium salt, was added to each well and incubated with cells. After incubation, the blue formazan crystals formed by metabolically active cells reducing the MTT reagent were solubilized, and the absorbance of the solution was measured at 562 nm using a microplate reader. The CellTiter-Glo® 2.0 Assay (Promega, Madison, WI, USA, G9242) measures ATP levels as an indicator of cell viability. Cells were plated in a multiwell plate and treated with ferroptosis inducers. The CellTiter-Glo reagent was added to each well, causing cell lysis and generating a luminescent signal proportional to the amount of ATP present. Luminescence was measured using a luminometer. The decrease in cell viability (%) was calculated using the following formula: 100 × (1 - (OD exp. mean value (- substrate blank)/OD control mean value (- substrate blank)).

Intracellular iron measurement

Intracellular iron concentrations in cells were determined by using the Iron Colorimetric Assay kit (Abcam, Cambridge, UK, ab83366), according to the manufacturer's instructions. For iron supplementation, we used ferric nitrate $Fe(NO_3)_3$ (Sigma, F8508) and ferrous sulfate $FeSO_4$ (Sigma, F8633) at a final concentration of 330 μM with the cell's corresponding medium supplemented with 0.5% fetal calf serum (Reactiva, 04-001-1A), MEM Non-Essential Amino Acids Solution (100 ×; ThermoFisher, Waltham, MA, USA, 11140050), 1 mM sodium pyruvate solution (Sigma, S8636), and 100 U/ml penicillin streptomycin (Gibco, Waltham, MA, USA, 15140122).

Statistical analysis

Data are shown as mean ± SEM. Results that were normally distributed (p >0.05 from the Kolmogorov–Smirnov test) were compared with parametric statistical procedures (two-tailed Student's t test and ANOVA followed by Bonferronis test for multiple comparisons). Non-normally distributed results were compared with non-parametric tests (Kruskall–Wallis one-way ANOVA and Mann–Whitney U test). Significance was accepted at p <0.05. The X^2 test was used to analyze the interaction between tumor-bearing status (incidence) and CPEB4 expression (WT or knockout). Sample sizes for reproducibility are indicated in the figure legends. Where representative images for immunohistochemical staining and immunoblot are shown, these results were independently observed at least three times. All *in vitro* experiments were repeated in at least three independent biological replicates. When possible, the investigators were blinded during experiments and outcome assessment.

Results

Low CPEB4 protein expression correlates with poor prognosis in human and mouse liver cancer

To evaluate the clinical significance of CPEB4 expression in human HCC, we performed a Kaplan–Meier survival analysis using publicly available data from the Human Protein Atlas. Our analysis showed that patients with low CPEB4 expression had significantly lower survival rates compared with those with high CPEB4 expression, indicating a strong association between reduced CPEB4 levels and poor prognosis (Fig. 1A).

In a mouse model of HFD-induced HCC, immunohistochemistry revealed minimal CPEB4 expression in normal liver tissue (Fig. 1B). Interestingly, CPEB4 levels increased during the precancerous stage of nodular hyperplasia but decreased as tumors progressed to more aggressive forms, such as adenomas and carcinomas (Fig. 1B). Histopathological analysis by expert pathologists, using standard H&E staining criteria, identified distinct features of these advanced stages. Carcinomas exhibited atypical cellular morphology, including irregular nuclei, variable cell size and shape, and disorganized, invasive growth patterns, accompanied by high mitotic activity. Additionally, they often showed necrosis, fibrosis, vascular invasion, and biliary ductular reactions. In contrast, adenomas had more organized architecture and lower mitotic activity, while nodular hyperplasia exhibited the least structural abnormalities.

These findings suggest that CPEB4 may play a protective role in liver tumorigenesis, with its upregulation during nodular hyperplasia potentially linked to liver regeneration and tumor suppression. The subsequent decline of CPEB4 during tumor progression could facilitate the shift from benign to malignant states, as evidenced by the increasing severity of histopathological features. Together, these results from both human and mouse models support the potential of CPEB4 as a prognostic marker and therapeutic target in liver cancer.

CPEB4 deficiency exacerbates HFD -associated liver cancer progression and aggressiveness

To investigate the causality of CPEB4 depletion in HFD-associated liver cancer, we utilized a global loss-of-function genetic mouse model ($CPEB4^{KO}$) on a C57BL/6J background, alongside WT controls. Male $CPEB4^{KO}$ and WT mice were subjected to a liver cancer protocol consisting of *ad libitum* HFD feeding (60% energy from fat), DEN injection (80 mg/kg), and phenobarbital supplementation (0.05% in the drinking water) (Fig. 1C). Control mice received the same treatment but were fed a standard ND (13% energy from fat). CPEB4 depletion in $CPEB4^{KO}$ mice was confirmed by immunoblotting (Fig. 1D). The liver cancer protocol was effective in inducing increased body weight (Fig. 1E), liver tumor growth (Fig. 1F–I), liver steatosis (Fig. 1J–L) and liver damage (Fig. 1M) in HFD-fed mice compared with ND-fed controls.

Interestingly, systemic depletion of CPEB4 intensified the tumorigenic phenotype in HFD-fed $CPEB4^{KO}$ mice, with increased liver tumor formation and aggressiveness (Fig. 1G–L) compared with HFD-fed WT mice. The exacerbated tumor development in $CPEB4^{KO}$ mice on HFD was not associated with enhanced liver steatosis (Fig. 1J) or significant differences in lipid accumulation (Fig. 1K and L) and transaminase levels (Fig. 1M) compared with HFD-fed WT mice. These findings suggest that CPEB4 plays a tumor-suppressive role under conditions of metabolic stress induced by HFD. Notably, both WT and $CPEB4^{KO}$ mice on an ND with DEN and phenobarbital exhibited minimal tumor burden (Fig. 1G and H), indicating that the loss of CPEB4 alone does not induce spontaneous liver tumor formation.

To further explore the role of CPEB4 in liver cancer, we generated a hepatocyte-specific CPEB4 knockout ($CPEB4^{HKO}$) by crossing $Cpeb4^{fl/fl}$ animals with Alb-Cre mice (Fig. 1N). Immunoblotting confirmed the absence of CPEB4 in the livers of $CPEB4^{HKO}$ mice (Fig. 1O). HFD feeding resulted in increased body weight in both $CPEB4^{HKO}$ and WT mice compared with mice on ND (Fig. 1P). Hepatocyte-specific CPEB4 loss under HFD conditions led to a more aggressive cancer phenotype, similar to that seen in globally CPEB4-deficient mice. $CPEB4^{HKO}$ mice showed a higher tumor number (Fig. 1G) and increased tumor aggressiveness (Fig. 1R) compared with WT mice on HFD.

These results highlight the critical protective role of CPEB4 in mitigating HFD-associated liver cancer, demonstrating that both systemic and hepatocyte-specific loss of CPEB4 exacerbate tumor progression under metabolic stress.

CPEB4 deficiency cell-autonomously increases the tumorigenic potential of liver cancer cells

To assess the intrinsic effects of CPEB4 depletion on the tumorigenic potential of liver cancer cells, we generated mice with tamoxifen-inducible CPEB4 deletion ($Cpeb4^{lox/lox}$; Ub-Cre-$ERT2^{+/+}$) (Fig. 2A). Following the induction of liver cancer through the pre-specified protocol (Fig. 1D), we isolated liver

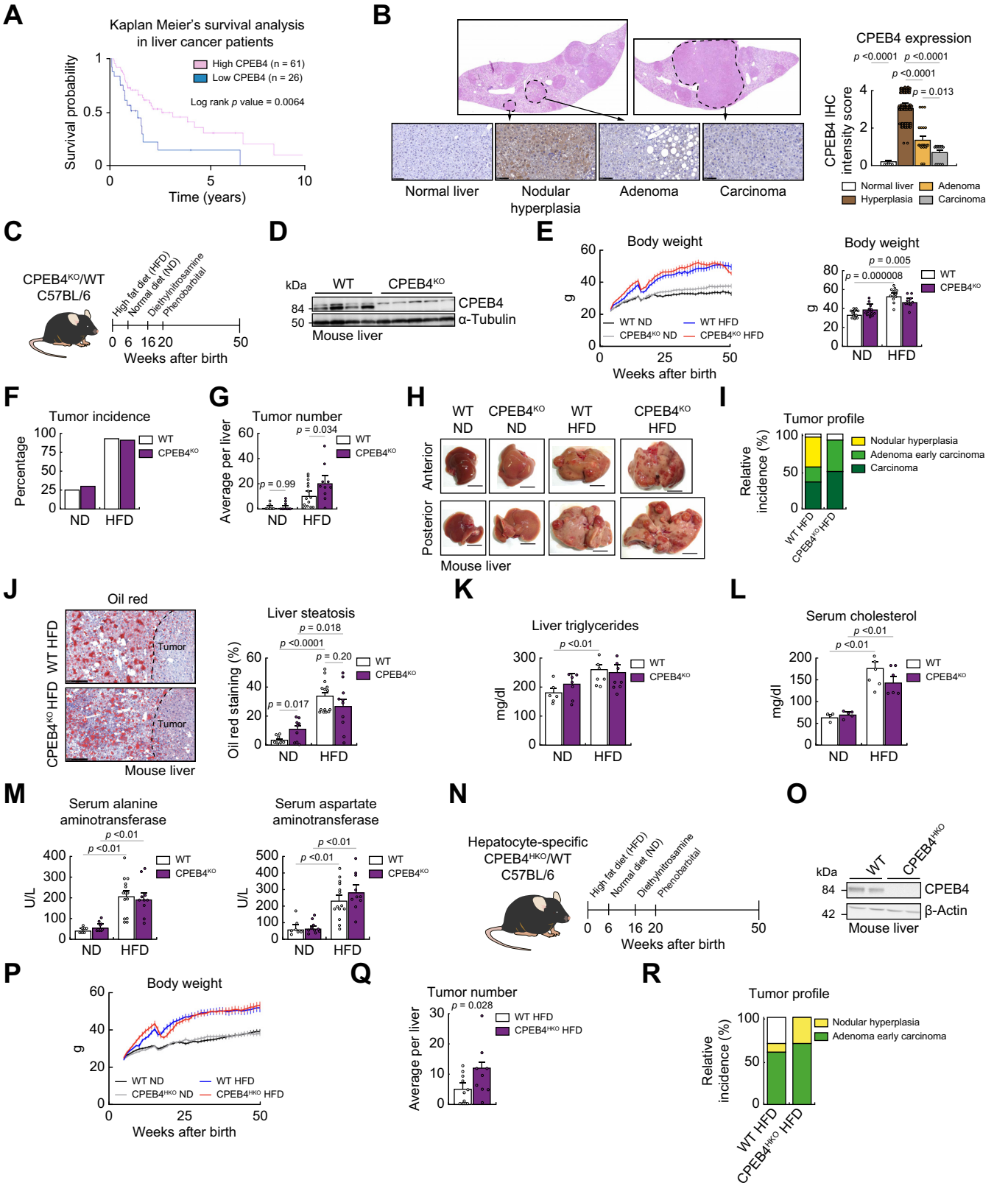

Fig. 1. CPEB4 depletion exacerbates high-fat diet-associated liver cancer progression and aggressiveness. (A) Kaplan–Meier analysis was used to compare overall survival between patients with liver cancer with high *vs.* low CPEB4 expression (n = 87). (B) Representative CPEB4 immunostainings in normal mouse liver and in the liver from WT mice fed high-fat diet (HFD), showing nodular hyperplasia, adenoma, and carcinoma. Scale bars, 100 μm. Semiquantitative immunohistochemical scoring of CPEB4 intensity on liver sections from wild-type (WT) mice fed HFD. H&E staining of the whole section of these livers is also shown. (C) Timeline of the experimental procedure to induce liver cancer in full body CPEB4^{KO} and WT mice (n = 10–15 mice per group). The mice were maintained on HFD or normal diet (ND)

tumors from these mice and generated a murine liver cancer cell line, termed 2020B4. Subsequent exposure of these cells to 1 μM tamoxifen induced CPEB4 depletion, as confirmed by immunoblotting (Fig. 2B). Control liver tumor cells retaining CPEB4 expression were exposed to the vehicle.

Consistent with a cell-autonomous anti-tumorigenic role for CPEB4, CPEB4^{KO} murine liver cancer cells exhibited significantly enhanced *in vitro* migratory capacity compared to WT controls (Fig. 2C). Moreover, CPEB4 depletion markedly increased the ability of these cells to form colonies in a 3D colony formation assay, as demonstrated through both an increased number and size of colonies in CPEB4^{KO} cells relative to WT cells (Fig. 2D).

Subsequent subcutaneous allograft and xenograft studies revealed a significantly higher tumor weight in CPEB4^{KO} liver cancer cells compared with WT cells, as indicated by increased tumor weight. This increased tumorigenic potential of the CPEB4-deficient tumors was observed in immunocompromised mice (Fig. 2E) and immunocompetent mice (Fig. 2F). To clarify this observation, we investigated whether CPEB4^{KO} increased tumor burden in orthotopic implantation models. Indeed, orthotopic transplantation of CPEB4^{KO}-luciferase liver cancer cells in immunocompromised (Fig. 2G) and immunocompetent mice (Fig. 2H) further corroborated these findings, allowing noninvasive monitoring of tumor growth using bioluminescence imaging.

To expand the relevance of our observations to human biology, we utilized the human liver cancer cell line HepG2 for xenograft mouse models. Using an shRNA-based approach, we downregulated CPEB4 expression in HepG2 cells (CPEB4^{KD}), and subsequently confirmed efficient silencing by immunoblotting (Fig. 2I). Strikingly, CPEB4 depletion in xenografted human tumors led to a robust pro-tumorigenic effect, as demonstrated by luminescence imaging (Fig. 2J). Collectively, these results emphasize the cell-autonomous role of CPEB4 as a pivotal negative regulator of the tumorigenic potential in both human and murine liver cancer cells.

Liver cancer aggravation upon CPEB4 deficiency was not associated with enhanced cell proliferation or reduced apoptotic or necroptotic cell death

To explore the mechanistic basis of our observations, we investigated whether alterations in cell proliferation or cell death contributed to the observed phenotype. Notably, the number of Ki67-positive proliferating cells in liver tumors of HFD-fed CPEB4^{HKO} mice exhibited no significant difference compared with their HFD-fed WT counterparts (Fig. 3A). Accordingly, the *in vitro* proliferative capacity of murine liver cancer cell lines, as demonstrated in 2D culture growth curves, remained unaltered upon CPEB4 depletion (Fig. 3B). Furthermore, *in vivo* allograft studies revealed no significant differences in the percentage of proliferating Ki67+ cells between CPEB4^{KO} and WT liver cancer cells (Fig. 3c). These findings suggest that the exacerbation of tumorigenicity in CPEB4^{KO} cells is not attributed to a direct mitogenic action of CPEB4 depletion.

In that perspective, we subsequently investigated whether the aggravation of liver cancer upon CPEB4 deletion was linked to decreased tumoral cell death. Terminal deoxynucleotidyl transferase dUTP nick-end labeling (TUNEL) revealed reduced cell death in the livers of HFD-fed CPEB4^{HKO} mice compared with WT mice (Fig. 3D). To determine the precise modality of cell death occurring, we first examined apoptosis given this has been at the forefront of academic research to date, as previously specified.[5] Liver tumors from HFD-fed CPEB4^{HKO} mice showed no significant reduction in apoptosis levels compared to WT mice, as demonstrated by the absence of differences in cleaved caspase-3 positive cells between the two groups based on immunohistochemistry (Fig. 3E). Immunoblotting further supported these results, showing consistent cleaved caspase-3 protein expression in the livers of HFD-fed CPEB4^{HKO} mice compared with WT mice (Fig. 3F). Notably, the percentage of cleaved caspase-3 positive cells in allograft tumors derived from CPEB4^{KO} mouse liver cancer cells mirrored that of tumors from WT liver cancer cells (Fig. 3G). Considering these results, apoptosis can be excluded as a factor in the reduced cell death observed in liver tumors following CPEB4 loss. Although the TUNEL assay is commonly used to detect apoptotic cell death by labeling fragmented DNA, it can also detect DNA fragmentation associated with other forms of cell death, such as necroptosis or ferroptosis.[29–31] Therefore, we investigated whether necroptosis or ferroptosis were affected by CPEB4 depletion. We observed no significant differences in the expression of the necroptosis marker phospho-mixed-lineage kinase-like domain (pMLKL)[32] between CPEB4-deficient and WT liver cancer cells, both in liver tumors (Fig. 3H) and allografted tumors (Fig. 3I). Additionally, the expression of receptor-interacting protein kinase-3 (RIPK3), which is essential for necroptosis,[33] did not change significantly when comparing CPEB4^{KO} and WT liver cancer cells (Fig. 3J). These findings suggest that another form of non-apoptotic and non-necroptotic cell death is reduced upon CPEB4 deletion in liver

from week 6 until sacrificed at 50 weeks of age. The hepatic carcinogen diethylnitrosamine (DEN, 80 mg/kg) was injected intraperitoneally into 16-week-old mice. From week 20 until the end of the protocol, 0.05% phenobarbital was added into the drinking water. (D) Immunoblotting for CPEB4 in the liver from CPEB4^{KO} and WT mice fed HFD, with α-tubulin as a loading control. The faint upper band represents an unspecific signal, while the lower band, absent in CPEB4^{KO} mice, reflects true CPEB4 expression. Such unspecific bands are consistent with previous studies,[46] and variations between blots may arise from differences in species, tissues, or antibody batches. (E) Body weight change over time (left) and final body weight at the age of 50 weeks (right) in CPEB4^{KO} and WT mice fed HFD or ND. (F) Tumor incidence, as percentage, in the liver from CPEB4^{KO} and WT mice fed HFD or ND. (G) Tumor number in the liver from CPEB4^{KO} and WT mice fed HFD or ND. (H) Representative macroscopic photographs of livers from CPEB4^{KO} and WT mice fed HFD or ND. Scale bar, 1 cm. (I) Tumor profile (nodular hyperplasia, adenoma, early carcinoma, and carcinoma) in the liver from CPEB4^{KO} and WT mice fed HFD. (J) Representative images (scale bar, 250 μm) and quantification of Oil Red-positive area (%) as an index of liver steatosis in the liver from CPEB4^{KO} and WT mice fed HFD or ND. (K) Liver triglyceride levels in CPEB4^{KO} and WT mice fed HFD or ND. (L) Serum cholesterol levels in CPEB4^{KO} and WT mice fed HFD or ND. (M) Serum alanine aminotransferase (left) and aspartate aminotransferase (right) in CPEB4^{KO} and WT mice fed HFD or ND. (N) Timeline of the experimental procedure to induce liver cancer in hepatocyte-specific CPEB4^{HKO} and WT mice (n = 9–12 mice per group). (O) Immunoblotting for CPEB4 in the liver from CPEB4^{HKO} and WT mice. β-Actin was used as loading control. (P) Body weight change over time in CPEB4^{HKO} and WT mice fed HFD or ND. (Q) Tumor number in the liver from CPEB4^{HKO} and WT mice fed HFD. (R) Tumor profile in the liver from CPEB4^{HKO} and WT mice fed HFD. All values represent mean ± SEM of biologically independent samples. Results that were normally distributed (p >0.05 from the Kolmogorov–Smirnov test) were compared with parametric statistical procedures (two-tailed Student's t test and ANOVA followed by Bonferroni's test for multiple comparisons). Non-normally distributed results were compared with non-parametric tests (Kruskall–Wallis one-way ANOVA and Mann–Whitney U test). Significance was accepted at p <0.05. In panel (F), the X^2 test was used to analyze the interaction between tumor-bearing status (incidence) and CPEB4 expression (WT or knockout). CPEB4, cytoplasmic polyadenylation element binding protein 4.

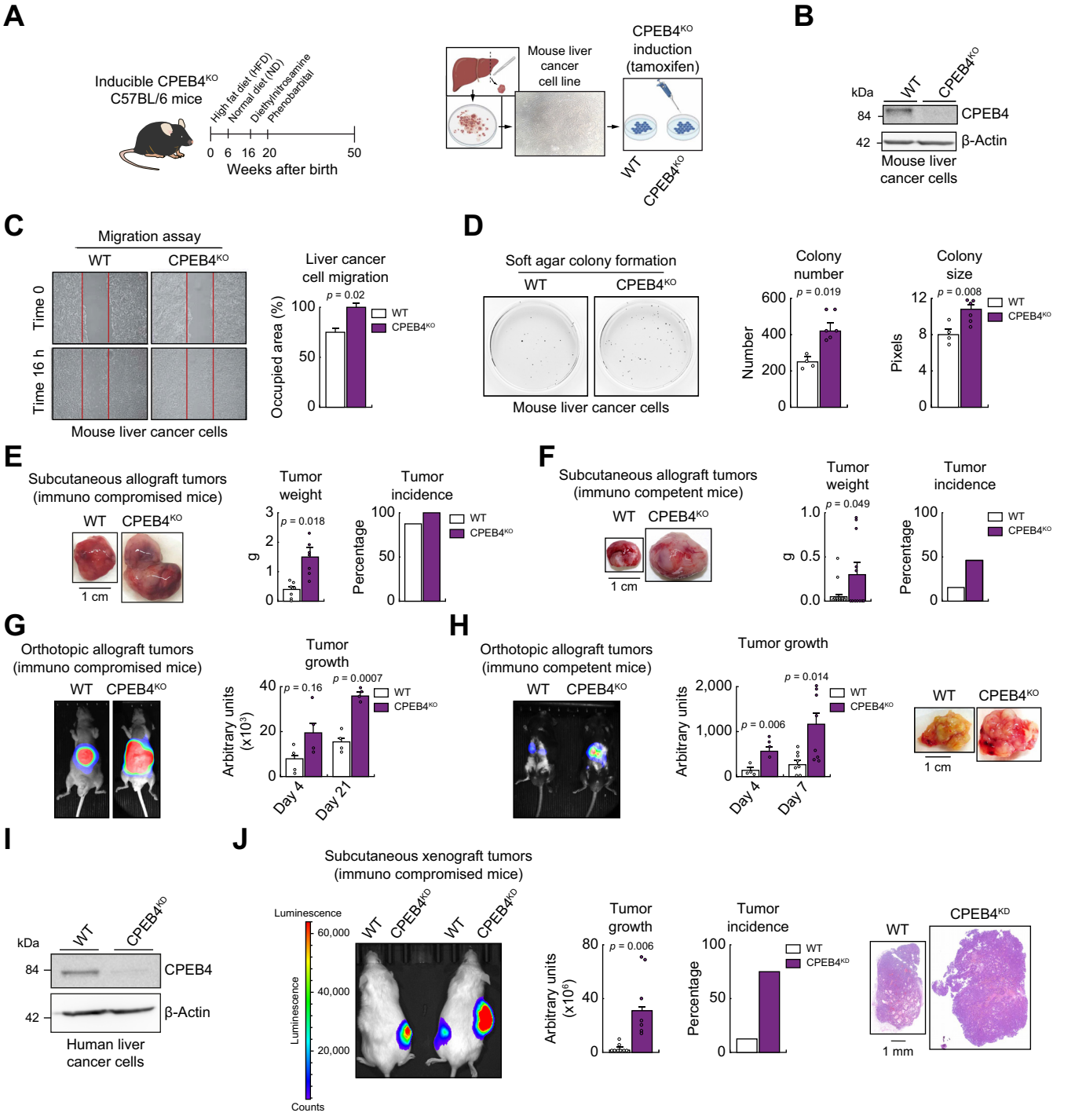

Fig. 2. CPEB4 depletion cell-autonomously increases the tumorigenic potential of liver cancer cells. (A) Generation of mouse liver cancer cell lines from inducible CPEB4 knockout (CPEB4^{KO}) mice. (B) Immunoblotting for CPEB4 in CPEB4^{KO} and wild-type (WT) mouse liver cancer cells. β-Actin was used as loading control. (C) Scratch wound-healing cell migration assay in CPEB4^{KO} and WT mouse liver cancer cells. Representative images were taken at 0 and 16 h. (D) Soft agar colony formation assay and quantification of colony number and size. (E) Tumor weight and incidence after subcutaneous implantation of CPEB4^{KO} and WT mouse liver cancer cells into immunocompromised nude mice. Representative macroscopic photographs of CPEB4^{KO} and WT tumors are shown. Scale bar, 1 cm. (F) Tumor weight and incidence after subcutaneous implantation of CPEB4^{KO} and WT mouse liver cancer cells into immunocompetent mice (the same tamoxifen-inducible mice used for generation of mouse tumor cell line). Representative macroscopic photographs of CPEB4^{KO} and WT tumors are shown. Scale bar, 1 cm. (G) Tumor growth, measured as luciferase signal, after orthotopic implantation of CPEB4^{KO} and WT mouse liver cancer cells into the livers of immunocompromised mice. Representative mouse photographs at day 21 after implantation are shown. (H) Tumor growth, measured as luciferase signal, after orthotopic implantation of CPEB4^{KO} and WT mouse liver cancer cells into livers of immunocompetent mice. Representative mouse photographs at day 4 after implantation, and macroscopic photographs of CPEB4^{KO} and WT tumors at endpoint are shown. Scale bar, 1 cm. (I) Immunoblotting for CPEB4 in CPEB4 knockdown (CPEB4^{KD}) and WT human liver cancer cells. β-Actin was used as loading control. (J) Tumor growth and incidence after subcutaneous implantation of CPEB4^{KD} and WT human HepG2 (ATCC®) liver cancer cells into severe combined immunodeficient SCID mice. Representative mouse photographs, and H&E-stained microscopic photographs of CPEB4^{KD} and WT tumors are shown. Scale bar, 1 mm. All values represent mean ± SEM of at least three biologically independent samples. Results that were normally distributed (p >0.05 from the Kolmogorov–

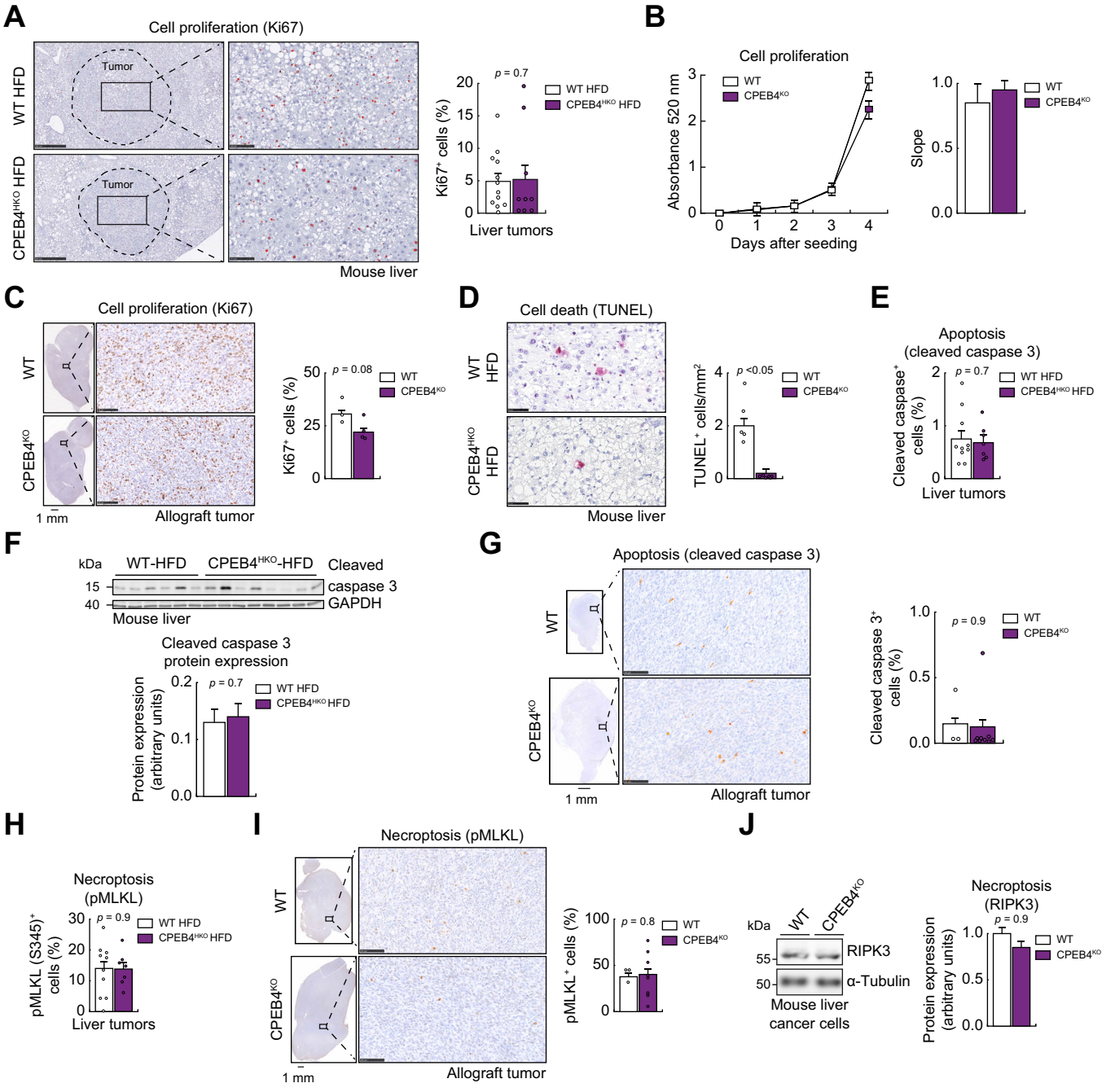

Fig. 3. Liver cancer aggravation upon CPEB4 depletion was not associated with enhanced cell proliferation or reduced apoptotic or necroptotic cell death. (A) Quantification of cell proliferation in mouse liver tumors based on Ki67 immunohistochemistry. Scale bars, 500 μm (low magnification) and 100 μm (high magnification). (B) Cell proliferation in mouse liver cancer cells. (C) Quantification of cell proliferation in allograft tumors based on Ki67 immunohistochemistry. Scale bars, 100 μm. (D) Cell death quantification in mouse liver tumors based on terminal deoxynucleotidyl transferase dUTP nick-end labeling (TUNEL) assay. Scale bars, 50 μm. (E) Quantification of apoptosis in mouse liver tumors based on immunohistochemistry for cleaved caspase 3. (F) Immunoblotting and quantification of cleaved caspase 3 in mouse liver. GAPDH was used as loading control. (G) Quantification of apoptosis in allograft tumors based on cleaved caspase 3 immunohistochemistry. Scale bars, 100 μm. (H) Quantification of necroptosis in mouse liver tumors based on immunohistochemistry for pMLKL. (I) Quantification of necroptosis in allograft tumors based on pMLKL immunohistochemistry. Scale bars, 100 μm. (J) Immunoblotting and quantification of the necroptosis marker RIPK3 in mouse liver cancer cells. α-Tubulin was used as loading control. All values represent mean ± SEM of at least three biologically independent samples. Results were compared with the two-tailed Student's *t* test. Significance was accepted at $p < 0.05$. CPEB4, cytoplasmic polyadenylation element binding protein 4.

Smirnov test) were compared with parametric statistical procedures (two-tailed Student's *t* test and ANOVA followed by Bonferroni's test for multiple comparisons). Non-normally distributed results were compared with non-parametric tests (Kruskall–Wallis one-way ANOVA and Mann–Whitney *U* test). Significance was accepted at $p < 0.05$. There were no significant differences in tumor incidence between CPEB4^{KO} and WT subcutaneous allograft tumors injected into immunocompromised mice (panel E) or immunocompetent mice (panel F), as determined using the X^2 test. CPEB4, cytoplasmic polyadenylation element binding protein 4.

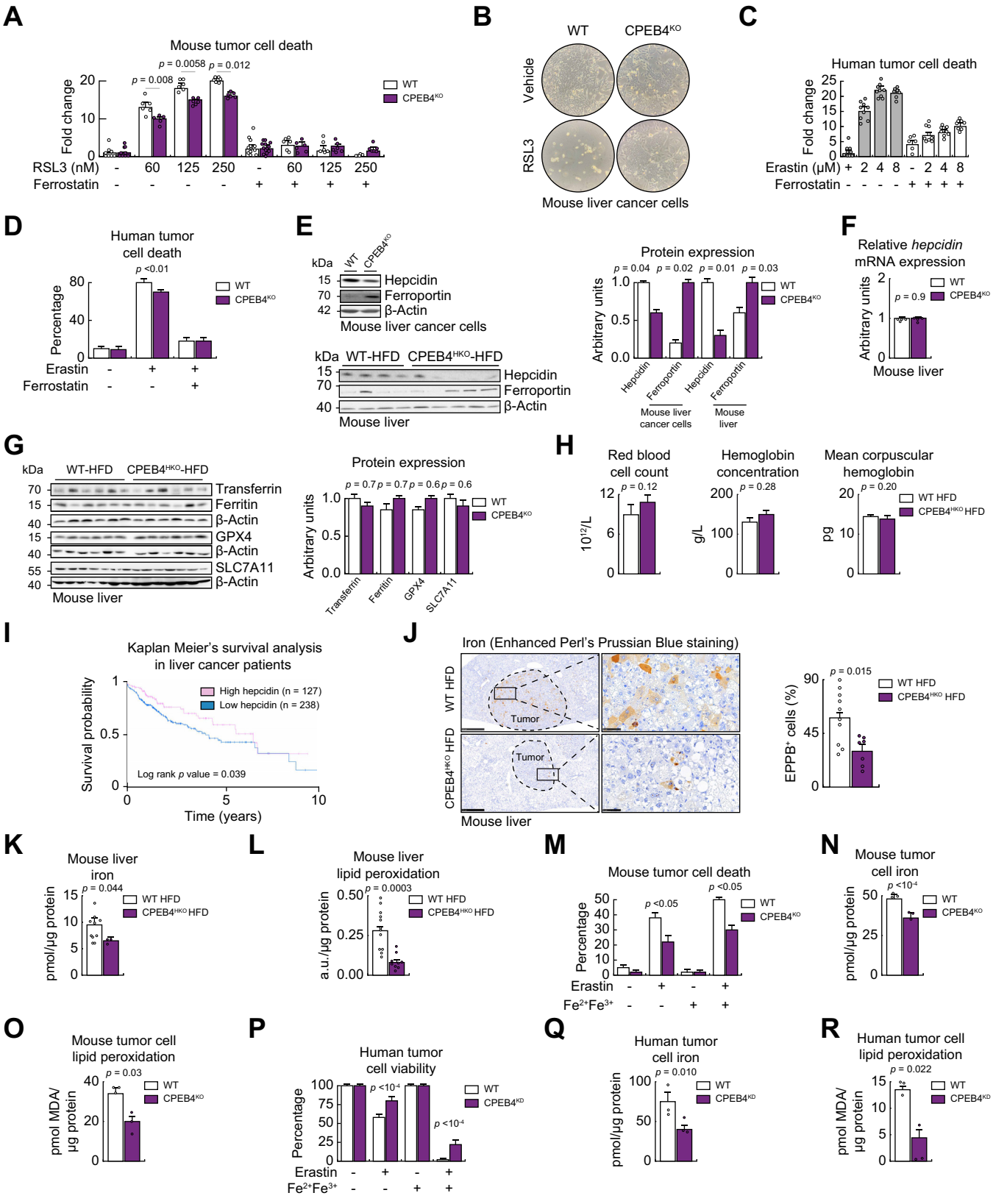

Fig. 4. CPEB4 deficiency decreases the susceptibility to iron-dependent ferroptotic cell death in liver cancer cells. (A) Cell death measurement in CPEB4^{KO} and wild-type (WT) mouse liver cancer cells after treatment with the ferroptosis inducer RSL3 for 24 h, with or without the ferroptosis-specific inhibitor ferrostatin-1 (5 μM). (B) Photographs of mouse liver cancer cells treated with 125 mM RSL3 for 24 h. (C) Cell death in WT human HepG2 liver cancer cells after treatment with erastin for 72 h, with or without 10 μM ferrostatin. (D) Cell death measurement in CPEB4^{KD} and WT human liver cancer cells after treatment with erastin, with or without ferrostatin. (E) Immunoblotting and protein expression quantification for hepcidin and ferroportin in mouse liver cancer cells and in the liver from CPEB4^{HKO} and WT

cancer cells, contributing to the exacerbation of liver cancer following CPEB4 depletion.

CPEB4 deficiency decreases the susceptibility of liver cancer cells to iron-dependent ferroptotic cell death

To investigate the mechanisms behind the exacerbation of HFD-related liver cancer upon CPEB4 depletion, we focused on ferroptosis, a recently identified form of non-apoptotic, non-necroptotic cell death characterized by iron-dependent lipid peroxide accumulation, resulting in lethal membrane damage.[6–9] We found that murine WT liver cancer cells are susceptible to ferroptotic cell death when treated with classical ferroptosis inducers,[34] RSL3 and erastin (Fig. 4A and B and Fig. S1A). This cell death was dose-dependent and confirmed as ferroptosis by its inhibition with ferroptosis inhibitors ferrostatin-1 and liproxstatin (Fig. 4A and B and Fig. S1A). Interestingly, CPEB4-depleted cells displayed reduced sensitivity to RSL3- and erastin-induced ferroptosis, an effect that was significantly reversed upon treatment with ferrostatin-1 or liproxstatin (Fig. 4A and B and Fig. S1A).

To substantiate these observations, we extended our analysis to human HepG2 liver cancer cells.[34] Consistent with murine liver cancer cells, erastin treatment induced substantial, dose-dependent cell death in HepG2 cells, with this effect being reduced by ferrostatin-1 (Fig. 4C). Notably, HepG2 cells with CPEB4 knockdown exhibited diminished sensitivity to erastin-induced ferroptosis compared with WT cells (Fig. 4D), an effect also attenuated by ferrostatin-1 (Fig. 4C and D). Similar findings were observed using another well-established human HCC cell line, Huh7 (Fig. 1B and C). These findings collectively reveal the susceptibility of liver cancer cells to ferroptotic cell death and establish the critical role of a CPEB4-dependent mechanism in regulating ferroptotic vulnerability in both human and murine liver cancer cells.

CPEB4 deficiency reduces hepcidin expression, leading to decreased iron accumulation and lipid peroxidation in liver cancer cells

To elucidate how CPEB4 depletion reduces the susceptibility of liver cancer cells to ferroptosis, we conducted an *in silico* analysis, building upon our previous publication.[20] Our objective was to identify direct mRNA targets of CPEB4 that might influence ferroptosis. Through this analysis, we identified HAMP, the gene encoding hepcidin, as a strong candidate because of its critical role in iron homeostasis and the execution of ferroptosis.[35] Notably, the 3′-UTR) of HAMP mRNA was found to be enriched in canonical CPE motifs (Fig. S1D), which we have previously shown to be binding sites for CPEB4.[20,21]

To verify the role of CPEB4 in regulating hepcidin, we measured hepcidin protein levels in CPEB4^{KO} mouse liver cancer cells, as well as in the livers of CPEB4^{HKO} mice fed an HFD (Fig. 4E). Immunoblotting revealed a significant reduction in hepcidin protein levels in CPEB4^{KO} liver cancer cells compared with WT cells (Fig. 4E). Similarly, HFD-fed CPEB4^{HKO} mice exhibited lower hepcidin protein expression in their livers compared with their HFD-fed WT counterparts (Fig. 4E). Interestingly, while hepcidin protein levels were notably downregulated in CPEB4-deficient tumor cells, RT-PCR analysis showed no corresponding change in hepcidin mRNA expression (Fig. 4F). Together, these results indicate that hepcidin production in liver cancer cells under stress conditions is, at least partially, regulated by CPEB4-dependent translation.

Hepcidin is involved in both iron homeostasis and ferroptosis induction by binding to and deactivating ferroportin, the primary iron exporter in mammalian cells.[35–37] In our study, we observed a correlation between reduced hepcidin levels and increased ferroportin protein expression in CPEB4^{KO} liver cancer cells and in the livers of HFD-fed CPEB4^{HKO} mice (Fig. 4E), as revealed by immunoblotting. Notably, the depletion of CPEB4 did not significantly affect the synthesis of transferrin and ferritin, which are additional components of the cellular iron-regulatory machinery (Fig. 4G). Furthermore, we did not observe significant changes in the expression of other ferroptosis-related proteins upon CPEB4 deletion, including glutathione peroxidase GPX4 and cystine/glutamate antiporter SLC7A11 (Fig. 4G).[38,39] This highlighted that liver cancer cells were protected from ferroptosis upon CPEB4 depletion by increasing iron export through modulation of the hepcidin–ferroportin pathway. Despite the decrease in hepcidin and increase in ferroportin, no significant alterations were observed in blood parameters dependent on iron, such as the number of circulating red blood cells, hemoglobin levels, or the mean corpuscular hemoglobin (Fig. 4H). However, it is important to note that CPEB4 depletion resulted in partial suppression of hepcidin rather than its complete absence (Fig. 4E). Therefore, it is not surprising that we did not observe the typical changes associated with diseases characterized by hepcidin deficiency or inappropriately high ferroportin activity, such as hereditary hemochromatosis.[40,41]

To address the clinical significance of hepcidin expression in human liver cancer, we conducted Kaplan–Meier survival analysis using data from the Human Protein Atlas. This analysis revealed that patients with low hepcidin expression had

mice fed HFD. β-Actin was used as loading control. Protein expression quantification of the immunoblots is shown. (F) Expression of hepcidin mRNA in the liver from CPEB4^{HKO} and WT mice fed HFD, measured by quantitative RT-PCR. (G) Immunoblotting and protein expression quantification for transferrin, ferritin, GPX4 and SLC7A11 in the liver from CPEB4^{HKO} and WT mice fed HFD. β-Actin was used as loading control. Protein expression quantification of the immunoblots is shown. (H) Red blood cell count, hemoglobin concentration and mean corpuscular hemoglobin in the blood from CPEB4^{HKO} and WT mice fed an HFD. (I) Kaplan–Meier analysis was used to compare overall survival between patients with liver cancer with high *vs.* low hepcidin expression (n = 365). (J) Quantification of iron in mouse liver tumors based on Enhanced Perl's Prussian Blue staining. (K) Iron levels in mouse liver cell lysate. Scale bars, 500 μm (low magnification) and 100 μm (high magnification). (L) Lipid peroxidation in mouse liver determined by using a Lipid Hydroperoxide (LPO) Assay Kit. (M) Cell death in mouse liver cancer cells after treatment with erastin and iron overload (ferric nitrate [$Fe(NO_3)_3$] and ferrous sulfate [$FeSO_4$] at a final concentration of 330 μM). (N) Iron levels in mouse liver cancer cells after iron overload. (O) Lipid peroxidation, assessed by malondialdehyde (MDA), in mouse liver cancer cells after treatment with 1 μM erastin for 24 h. (P) Cell viability measurement in human liver cancer cells. (Q) Iron in human liver cancer cells after iron overload. (R) Lipid peroxidation (MDA) in human liver cancer cells after treatment with 1 μM erastin for 24 h. All values represent mean ± SEM of at least three biologically independent samples. Results that were normally distributed (p >0.05 from the Kolmogorov–Smirnov test) were compared with parametric statistical procedures (two-tailed Student's t test and ANOVA followed by Bonferroni's test for multiple comparisons). Non-normally distributed results were compared with non-parametric tests (Kruskall–Wallis one-way ANOVA and Mann–Whitney U test). Significance was accepted at p <0.05. CPEB4, cytoplasmic polyadenylation element binding protein 4.

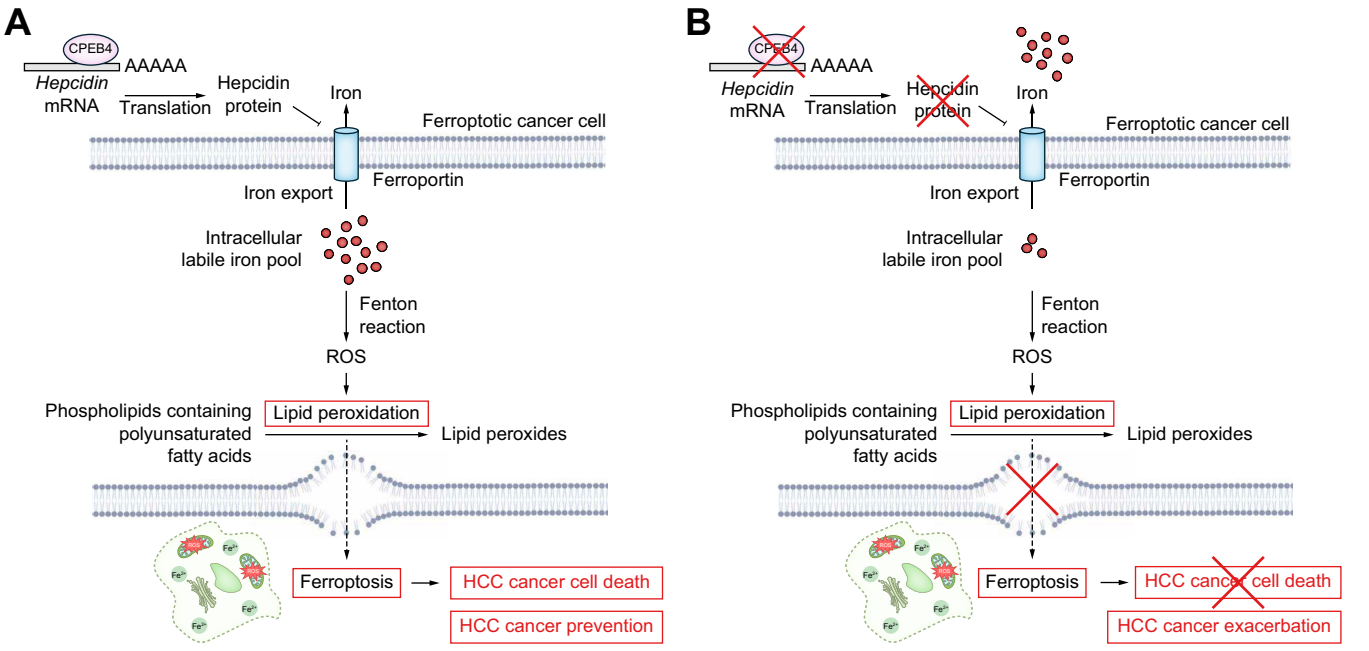

Fig. 5. Role of CPEB4 in regulating ferroptosis and HCC cancer cell fate. (A) CPEB4-mediated hepcidin expression and HCC cancer prevention: In the presence of CPEB4, the translation of *hepcidin* mRNA into hepcidin protein is promoted. Hepcidin protein binds to ferroportin, a cellular iron exporter, leading to its internalization and degradation. This results in an accumulation of intracellular labile iron, which undergoes the Fenton reaction to produce reactive oxygen species (ROS). ROS induce lipid peroxidation of phospholipids containing polyunsaturated fatty acids, generating lipid peroxides and triggering ferroptosis. Ferroptosis leads to cancer cell death and contributes to cancer attenuation and prevention. (B) CPEB4 deficiency and HCC cancer exacerbation: under conditions of CPEB4 deficiency, the translation of *hepcidin* mRNA into protein is attenuated. Consequently, ferroportin remains active on the cell surface, facilitating iron export from the cell. This prevents the accumulation of intracellular labile iron, reducing ROS production and lipid peroxidation. Without sufficient lipid peroxidation, ferroptosis is inhibited, leading to reduced cancer cell death and potentially exacerbating cancer progression. CPEB4, cytoplasmic polyadenylation element binding protein 4; HCC, hepatocellular carcinoma.

significantly lower survival rates compared with those with high hepcidin expression, indicating that reduced hepcidin levels are associated with poorer prognosis. This finding aligns with our own survival analysis results for CPEB4 (Fig. 4I).

To assess the functional consequences of hepcidin downregulation and ferroportin upregulation following CPEB4 depletion, we evaluated intracellular iron content. Quantitative analysis of Enhanced Perl's Prussian Blue histological stainings revealed diminished intracellular iron stores in liver tumors of HFD-fed CPEB4^{HKO} mice compared with WT counterparts (Fig. 4J). Furthermore, biochemical analyses confirmed significantly reduced intracellular iron levels in the livers of HFD-fed CPEB4^{HKO} mice compared with HFD-fed WT mice (Fig. 4K). Concurrently, iron-dependent lipid peroxidation, a functional marker of ferroptosis, was notably reduced in the livers of HFD-fed CPEB4^{HKO} mice, as indicated by decreased levels of lipid hydroperoxide, corresponding with the decrease in iron levels (Fig. 4L).

To further investigate the impact of intracellular iron levels on CPEB4-mediated regulation of ferroptosis, we conducted experiments under conditions of iron overload by treating tumoral cells with a combination of ferric nitrate ($Fe(NO_3)_3$) and ferrous sulfate ($FeSO_4$) at a final concentration of 330 μM. We observed that inducing ferroptosis with erastin in murine liver cancer cells under conditions of iron excess resulted in increased levels of cell death (Fig. 4M). Remarkably, cells lacking CPEB4 exhibited lower levels of cell death compared with WT cells when exposed to erastin under conditions of iron overload. This reduced susceptibility to ferroptosis in CPEB4-deficient cells was associated with lower intracellular iron levels (Fig. 4N) and decreased lipid peroxidation (Fig. 4O) compared with WT liver cancer cells. We further validated these findings using human liver cancer cells (Fig. 4P–R). Collectively, these results indicate that tumoral cells lacking CPEB4 can better maintain lower intracellular iron levels because of reduced levels of hepcidin. Consequently, this leads to increased ferroportin expression and enhanced export of iron outside the cell, ultimately reducing lipid peroxidation and susceptibility to ferroptosis (Fig. 5). Taken together, these findings provide compelling evidence supporting the role of CPEB4 in regulating intracellular iron levels and susceptibility to ferroptosis.

Discussion

This study underscores the critical role of CPEB4-regulated translation in HCC, revealing how CPEB4 influences the susceptibility of liver cancer cells to ferroptosis, an essential tumor suppression mechanism. Evading regulated cell death is a hallmark of cancer progression, underscoring the importance of these findings in understanding HCC biology.

Our analysis identified that low CPEB4 protein expression is linked to poor prognosis in both human and mouse HCC models. Kaplan–Meier survival data from the Human Protein Atlas demonstrated a significant association between lower CPEB4 levels and reduced survival in patients with liver cancer.

Immunohistochemistry further supported these findings, showing that liver tumors with diminished CPEB4 expression exhibited increased severity in a mouse model of HFD-related liver cancer. Whole-body and hepatocyte-specific CPEB4 deficiencies exacerbated HFD-associated liver cancer progression, emphasizing the tumor-suppressive function of CPEB4 in this context and highlighting its potential as a therapeutic target. Additionally, our findings indicate that CPEB4 deficiency promotes the tumorigenic capacity of liver cancer cells through enhanced migration and colony formation *in vitro*. Consistently, allograft, xenograft, and orthotopic implantation studies showed increased tumorigenic potential in CPEB4-depleted liver cancer cells in both murine and human models. This reinforces the notion that CPEB4 acts as a crucial cell-autonomous regulator, where its presence suppresses tumorigenicity, and its deficiency fosters HCC development and progression.

The increased aggressiveness seen with CPEB4 depletion was not associated with alterations in cell proliferation, apoptosis, or necroptosis. Instead, our findings indicate that liver tumor cells lacking CPEB4, both in human and mouse models, exhibit reduced sensitivity to iron-ferroptotic cell death. Ferroptosis, a regulated cell death mechanism driven by iron-induced lipid peroxidation, relies on iron to propagate lipid peroxidation and activate iron-dependent enzymes, including lipoxygenases.[6–9,34] Importantly, our study identified hepcidin as a direct mRNA target of CPEB4, with CPEB4 enhancing hepcidin translation under cellular stress conditions. In both CPEB4-deficient liver cancer cells and HFD-fed CPEB4^{HKO} mice, we observed reduced hepcidin levels, elevated ferroportin expression, lower intracellular iron, decreased lipid peroxidation, and consequently diminished susceptibility to ferroptosis. Ferroportin, the primary cellular iron export channel, is regulated by hepcidin; hepcidin binding to ferroportin initiates its internalization and degradation.[35–37] Despite the observed reduction in hepcidin and corresponding increase in ferroportin, we noted no significant alterations in systemic iron-related blood parameters, such as circulating red blood cell count, hemoglobin levels, or mean corpuscular hemoglobin. Notably, CPEB4 depletion under HFD conditions only partially reduced hepcidin rather than completely abolishing it, explaining the absence of classic symptoms associated with hepcidin deficiency or excessive ferroportin activity, such as those seen in hereditary hemochromatosis.[40,41]

Overall, these findings emphasize the importance of CPEB4-regulated translation in modulating ferroptotic responses via hepcidin synthesis and intracellular iron balance. They further underline ferroptosis resistance as a key driver of liver cancer progression.[42,43] Our data suggest that, when ferroptotic mechanisms are intact (*i.e.* in the presence of CPEB4), ferroptosis limits liver cancer progression (Fig. 5A). Conversely, CPEB4 deficiency impairs this machinery, giving liver cancer cells a selective advantage and driving tumor aggressiveness (Fig. 5B). This interpretation is consistent with our findings that CPEB4-deficient liver cancer cells exhibit disturbances in iron metabolism, reduced ferroptosis sensitivity, and enhanced tumorigenicity.

Our results are also in line with previous studies that describe the dynamic and stage-specific expression of CPEB4 in HCC. CPEB4 downregulation has been linked to miRNA-550a, promoting migration and invasion and correlating with poorer prognosis in HCC.[44] Moreover, CPEB4 shows a biphasic expression pattern: high in early HCC and reduced in advanced tumors,[45] supporting our observations that CPEB4 deficiency fosters aggressive tumor characteristics and reduced ferroptosis susceptibility, suggesting an additional tumor-suppressive mechanism.

Interestingly, our previous research found elevated CPEB4 in regenerative micronodules of cirrhotic liver, suggesting a role in liver regeneration.[46] In our current study, nodular hyperplasia also showed increased CPEB4, potentially because of regenerative activity. However, CPEB4 levels declined as tumors progressed, indicating a transition from a regenerative to a pathological state. This fluctuating expression pattern of CPEB4 in liver carcinogenesis underscores its complex, stage-specific, and cell-context-dependent functions in liver pathology.[47,48] Given the heterogeneity of liver cancer, the impact of CPEB4 on tumor behavior and iron metabolism may vary across HCC subtypes, potentially limiting the generalizability of these findings. Future studies should explore the role of CPEB4 across diverse HCC subtypes to enhance understanding of its context-dependent functions and assess its therapeutic relevance.

In summary, our study suggests that CPEB4 modulates HCC progression by regulating ferroptosis and iron homeostasis. Therapeutically, activating CPEB4 in tumor cells via phosphorylation could represent a novel approach for HCC treatment.[49] Furthermore, because CPEB4 is antagonized by CPEB1,[19,49,50] increasing CPEB4 activity might be achievable through CPEB1 inhibition. Early-stage development of small molecule inhibitors targeting CPEB1 is underway, which may help elevate CPEB4 levels and reveal potential clinical benefits.

Affiliations

[1]*FRCB-IDIBAPS Biomedical Research Institute; Barcelona, Spain;* [2]*Institute for Research in Biomedicine (IRB), The Barcelona Institute of Science and Technology, Barcelona, Spain;* [3]*Institució Catalana de Recerca i Estudis Avançats (ICREA); Barcelona, Spain*

Abbreviations

CPE, cytoplasmic polyadenylation element; CPEB, cytoplasmic polyadenylation element binding protein; CPEB4, cytoplasmic polyadenylation element binding protein 4; DEN, diethylnitrosamine; HCC, hepatocellular carcinoma; HFD, high-fat diet; MAFLD, metabolic-associated fatty liver disease; MDA, malondialdehyde; MTT, 3-(4,5-dimethylthiazol-2-yl)-2,5-diphenyltetrazolium bromide; ND, normal diet; pMLKL, phospho-mixed-lineage kinase-like domain; RIPK3, receptor-interacting protein kinase-3; ROS, reactive oxygen species; shRNA, short hairpin RNA; TUNEL, terminal deoxynucleotidyl transferase dUTP nick-end labeling; UTR, untranslated region.

Financial support

This work was supported by grants from the Spanish Ministry of Science, Innovation and Universities (SAF2017-87988-R, PID2020-118937RB-I00, PID2023-150033OB-I00, PRE2018-083718, PRE2021-100657 and RED2022-134485-T to MF; PID2020-119533GB-I00 and PDC2021-121716-I00 to RM), and the Spanish Association Against Cancer (GCB15152955MEND and PRYCO234903AZNA), Worldwide Cancer Research Foundation (20_0284), World Cancer Research Fund International (IIG_FULL_2020_021; funding obtained from Wereld Kanker Onderzoek Fonds [WKOF]), BBVA Foundation (28/2019), La Caixa Foundation

(HR18-00302), La Marat TV3 Foundation (2019-0259) and the Government of Catalonia (2021-SGR-01321 and BP19-00040) to MF and RM. IDIBAPS and IRB are supported by the CERCA Programme (Catalan Government). IRB is the recipient of a Severo Ochoa Award of Excellence from the Spanish Government. MED had a Beatriu de Pinos postdoctoral fellowship from the Government of Catalonia. We also thank N. Prats from the Histopathology Facility at IRB for their assistance with analysis.

Conflicts of interest

The authors declare no competing interests.

Please refer to the accompanying ICMJE disclosure forms for further details.

Authors' contributions

Acquisition of data: MED, SNS, MRP, BIC, CGM, AB, EB, JM, MB, MF. Analysis of data: MED, SNS, MRP, BIC, CGM. Study concept, design, and supervision: MF. Scientific input: RM. Writing of manuscript and design of figures: MF. Funding acquisition: RM, MF.

Data availability statement

All data associated with this work are presented in the main manuscript or Supplementary material. For availability of any other type of data, contact the corresponding authors.

Supplementary data

Supplementary data to this article can be found online at https://doi.org/10.1016/j.jhepr.2024.101296.

References

Author names in bold designate shared co-first authorship

[1] Villanueva A. Hepatocellular carcinoma. N Engl J Med 2019;380:1450–1462.
[2] Calle EE, Kaaks R. Overweight, obesity and cancer: epidemiological evidence and proposed mechanisms. Nat Rev Cancer 2004;4:579–591.
[3] Llovet JM, Willoughby CE, Singal AG, et al. Nonalcoholic steatohepatitis-related hepatocellular carcinoma: pathogenesis and treatment. Nat Rev Gastroenterol Hepatol 2023;20:487–503.
[4] **Anstee QM**, **Reeves HL**, Kotsiliti E, et al. From NASH to HCC: current concepts and future challenges. Nat Rev Gastroenterol Hepatol 2019;16:411–428.
[5] **Strasser A**, **Vaux DL**. Cell death in the origin and treatment of cancer. Mol Cell 2020;78:1045–1054.
[6] Stockwell BR, Friedmann Angeli JP, Bayir H, et al. Ferroptosis: a regulated cell death nexus linking metabolism, redox biology, and disease. Cell 2017;171:273–285.
[7] Dixon SJ, Lemberg KM, Lamprecht MR, et al. Ferroptosis: an iron-dependent form of nonapoptotic cell death. Cell 2012;149:1060–1072.
[8] **Jiang X**, **Stockwell BR**, **Conrad M**. Ferroptosis: mechanisms, biology and role in disease. Nat Rev Mol Cell Biol 2021;22:266–282.
[9] Chen X, Kang R, Kroemer G, et al. Broadening horizons: the role of ferroptosis in cancer. Nat Rev Clin Oncol 2021;18:280–296.
[10] Silvera D, Formenti SC, Schneider RJ. Translational control in cancer. Nat Rev Cancer 2010;10:254–266.
[11] Robichaud N, Sonenberg N. Translational control and the cancer cell response to stress. Curr Opin Cell Biol 2017;45:102–109.
[12] Bhat M, Robichaud N, Hulea L, et al. Targeting the translation machinery in cancer. Nat Rev Drug Discov 2015;14:261–278.
[13] Truitt ML, Ruggero D. New frontiers in translational control of the cancer genome. Nat Rev Cancer 2016;16:288–304.
[14] Truitt ML, Conn CS, Shi Z, et al. Differential requirements for eIF4E dose in normal development and cancer. Cell 2015;162:59–71.
[15] Weill L, Belloc E, Bava FA, et al. Translational control by changes in poly(A) tail length: recycling mRNAs. Nat Struct Mol Biol 2012;19:577–585.
[16] Fernandez-Miranda G, Mendez R. The CPEB-family of proteins, translational control in senescence and cancer. Ageing Res Rev 2012;11:460–472.
[17] Belloc E, Mendez R. A deadenylation negative feedback mechanism governs meiotic metaphase arrest. Nature 2008;452:1017–1021.
[18] Ivshina M, Lasko P, Richter JD. Cytoplasmic polyadenylation element binding proteins in development, health, and disease. Annu Rev Cell Dev Biol 2014;30:393–415.
[19] Bava FA, Eliscovich C, Ferreira PG, et al. CPEB1 coordinates alternative 3'UTR formation with translational regulation. Nature 2013;495:121–125.
[20] Pique M, Lopez JM, Foissac S, et al. A combinatorial code for CPE-mediated translational control. Cell 2008;132:434–448.
[21] Novoa I, Gallego J, Ferreira PG, et al. Mitotic cell cycle progression is regulated by CPEB-dependent translational control. Nat Cell Biol 2010;12:447–456.
[22] Fernandez-Alfara M, Sibilio A, Martin J, et al. Antitumor T-cell function requires CPEB4-mediated adaptation to chronic endoplasmic reticulum stress. EMBO J 2023;42:e111494.
[23] Maillo C, Martin J, Sebastian D, et al. Circadian- and UPR-dependent control of CPEB4 mediates a translational response to counteract hepatic steatosis under ER stress. Nat Cell Biol 2017;19:94–105.
[24] Ortiz-Zapater E, Pineda D, Martinez-Bosch N, et al. Key contribution of CPEB4-mediated translational control to cancer progression. Nat Med 2011;18:83–90.
[25] Parras A, Anta H, Santos-Galindo M, et al. Autism-like phenotype and risk gene mRNA deadenylation by CPEB4 mis-splicing. Nature 2018;560:441–446.
[26] Perez-Guijarro E, Karras P, Cifdaloz M, et al. Lineage-specific roles of the cytoplasmic polyadenylation factor CPEB4 in the regulation of melanoma drivers. Nat Commun 2016;7:13418.
[27] Riechert E, Kmietczyk V, Stein F, et al. Identification of dynamic RNA-binding proteins uncovers a Cpeb4-controlled regulatory cascade during pathological cell growth of cardiomyocytes. Cell Rep 2021;35:109100.
[28] Sibilio A, Suñer C, Fernandez-Alfara M, et al. Immune translational control by CPEB4 regulates intestinal inflammation resolution and colorectal cancer development. iScience 2022;25:103790.
[29] Moore CL, Savenka AV, Basnakian AG. TUNEL assay: a powerful tool for kidney injury evaluation. Int J Mol Sci 2021;22:412.
[30] Zhu Y, Cui H, Xia Y, et al. RIPK3-mediated necroptosis and apoptosis contributes to renal tubular cell progressive loss and chronic kidney disease progression in rats. PLoS One 2016;11:e0156729.
[31] Su L, Jiang X, Yang C, et al. Pannexin 1 mediates ferroptosis that contributes to renal ischemia/reperfusion injury. J Biol Chem 2019;294:19395–19404.
[32] Murphy JM, Czabotar PE, Hildebrand JM, et al. The pseudokinase MLKL mediates necroptosis via a molecular switch mechanism. Immunity 2013;39:443–453.
[33] **Mompean M**, **Li W**, **Li J**, et al. The structure of the necrosome RIPK1–RIPK3 core, a human hetero-amyloid signaling complex. Cell 2018;173:1244–1253.
[34] **Conrad M**, **Pratt DA**. The chemical basis of ferroptosis. Nat Chem Biol 2019;15:1137–1147.
[35] Nemeth E, Tuttle MS, Powelson J, et al. Hepcidin regulates cellular iron efflux by binding to ferroportin and inducing its internalization. Science 2004;306:2090–2093.
[36] Donovan A, Lima CA, Pinkus JL, et al. The iron exporter ferroportin/Slc40a1 is essential for iron homeostasis. Cell Metab 2005;1:191–200.
[37] Qiao B, Sugianto P, Fung E, et al. Hepcidin-induced endocytosis of ferroportin is dependent on ferroportin ubiquitination. Cell Metab 2012;15:918–924.
[38] **Yang WS**, **SriRamaratnam R**, Welsch ME, et al. Regulation of ferroptotic cancer cell death by GPX4. Cell 2014;156:317–331.
[39] **Zhang W**, **Sun Y**, **Bai L**, et al. RBMS1 regulates lung cancer ferroptosis through translational control of SLC7A11. J Clin Invest 2021;131:e152067.
[40] Fernandes A, Preza GC, Phung Y, et al. The molecular basis of hepcidin-resistant hereditary hemochromatosis. Blood 2009;114:437–443.
[41] Lesbordes-Brion JC, Viatte L, Bennoun M, et al. Targeted disruption of the hepcidin 1 gene results in severe hemochromatosis. Blood 2006;108:1402–1405.
[42] Sun X, Ou Z, Chen R, et al. Activation of the p62-Keap1-NRF2 pathway protects against ferroptosis in hepatocellular carcinoma cells. Hepatology 2016;63:173–184.
[43] **Zhu R**, **Gao C**, **Feng Q**, et al. Ferroptosis-related genes with post-transcriptional regulation mechanisms in hepatocellular carcinoma determined by bioinformatics and experimental validation. Ann Transl Med 2022;10:1390.
[44] Tian Q, Liang L, Ding J, et al. MicroRNA-550a acts as a pro-metastatic gene and directly targets cytoplasmic polyadenylation element-binding protein 4 in hepatocellular carcinoma. PLoS One 2012;7:e48958.
[45] **Tsai LY**, **Chang YW**, Lee MC, et al. Biphasic and stage-associated expression of CPEB4 in hepatocellular carcinoma. PLoS One 2016;11:e0155025.
[46] **Calderone V**, **Gallego J**, Fernandez-Miranda G, et al. Sequential functions of CPEB1 and CPEB4 regulate pathologic expression of vascular endothelial

growth factor and angiogenesis in chronic liver disease. Gastroenterology 2016;150:982–997.
[47] Mejias M, Gallego J, Naranjo-Suarez S, et al. CPEB4 increases expression of PFKFB3 to induce glycolysis and activate mouse and human hepatic stellate cells, promoting liver fibrosis. Gastroenterology 2020;159:273–288.
[48] Pell N, Garcia-Pras E, Gallego J, et al. Targeting the cytoplasmic polyadenylation element-binding protein CPEB4 protects against diet-induced obesity and microbiome dysbiosis. Mol Metab 2021;54:101388.
[49] **Duran-Arque B**, **Cañete M**, Castellazzi CL, et al. Comparative analyses of vertebrate CPEB proteins define two subfamilies with coordinated yet distinct functions in post-transcriptional gene regulation. Genome Biol 2022;23:1–27.
[50] Guillen-Boixet J, Buzon V, Salvatella X, et al. CPEB4 is regulated during cell cycle by ERK2/Cdk1-mediated phosphorylation and its assembly into liquid-like droplets. Elife 2016;5:e19298.

Keywords: Translation; Cytoplasmic polyadenylation element binding protein; Ferroptotic cell death; Hepatocellular carcinoma.
Received 17 July 2024; received in revised form 3 December 2024; accepted 4 December 2024; Available online 12 December 2024